Generalized coherent-squeezed-state expansion for the super-radiant phase transition

Xiang-You Chen,[1,2] Yu-Yu Zhang,[1,3,*] Libin Fu,[3] and Hang Zheng[4,5,†]
[1]*Department of Physics, Chongqing University, Chongqing 401330, China*
[2]*Department of Physics, Zhejiang University, Hangzhou 310027, China*
[3]*Graduate School, China Academy of Engineering Physics, Beijing 100193, China*
[4]*Department of Physics and Astronomy, Shanghai Jiaotong University, Shanghai 200240, China*
[5]*Beijing Computational Science Research Center, Beijing 100193, China*

(Received 30 August 2019; revised manuscript received 22 November 2019; accepted 18 February 2020; published 18 March 2020)

We develop a coherent-squeezed-state expansion for the ground state of the quantum phase transition in the quantum Rabi model. The wave function undergoes a transition from a localized state in the normal phase to a two-peaks delocalized state in the super-radiant phase. Interestingly, the two displaced wave packets are squeezed in the momentum space, and overlap strongly to form a correlated state. We develop a superposition of coherent-squeezed states to describe the phase transition correctly, which includes the higher-order excitations at the critical value. The corresponding ground-state energy and the average photon number are in agreement with numerical ones, exhibiting an improvement over previous coherent-state expansions. Moreover, our method successfully captures the reduced quantum fluctuations in momentum variable in the phase transition.

DOI: 10.1103/PhysRevA.101.033827

I. INTRODUCTION

Quantum Rabi model (QRM) describes the interactions of a two-level atom with a single mode of the quantized electromagnetic field (EMF) [1]. It has a wide application in cavity QED [2,3] and circuit QED [4–9] to simulate the strong coupling of the two-level systems and the EMF. Recently, an emergence of quantum phase transition is found in the QRM when a ratio of the atomic transition frequency Δ to the field frequency ω approaches infinity, $\Delta/\omega \to \infty$ [10–12]. In this limit, the system undergoes a super-radiant phase transition (SPT), which is the same type of the SPT associated with collective behavior in the Dicke model in the thermodynamics limit [13–17]. There are ongoing efforts on the critical properties, the scaling exponents, and the universality to understand the SPT in the quantum Rabi model. However, the nature of the wave function has received little attention due to the strong-correlated physics of the quantum phase transition.

The complexity of the wave function comes from the absence of the closed-form basis sets since the excitation number is not conserved. The need for an exact solution is especially amplified in understanding the phase transition. For the super-radiant phase, higher-order excitations for the multiphoton process is required even in this linear one-photon coupling system, which induces the effective nonlinear interactions. In previous studies, one can find the higher-order terms should be considered in the expansion of the exact solution with complicated transcendental functions [18–20]. The previous coherent-state (CS) approaches [21–26] with only the displacement transformation is not sufficient to describe the effective nonlinear effects for a strong coupling. The unknown squeeze effects, which usually occur in two-photon nonlinear coupling systems [27–29], are expected to play a crucial role in the one-photon QRM for the higher-order excitations. As an improvement, a coherent-squeezed-state (CSS) approach has been proposed to capture the additional squeezing effects [30–34], which are neglected in the CS basis. The other difficulty of the wave-function ansatz is the emergence of strong correlation physics in the critical coupling regime. As the coupling strength increases, it was found that the ground state of the QRM was a superposition of a set of correlated polaron states [35–37]. It means that higher-order expansions of the wave function are required in the phase transition. It is worthwhile to discuss possible extensions of the CSS technique in describing the ground state of the system through the phase transition.

Here we explore an expansion of the CSS to capture the displacement and squeezing deformations of the wave function in the phase transition. Using the Wigner function, the wave function is found to be localized with one peak in the normal phase, and then appears as two peaks with two different displacements to form a delocalized state in the super-radiant phase. Around the critical regime, the wave packets are squeezed in the momentum space and become strongly correlated. Fortunately, the strong-correlated state is well described by the superposition of two coherent-squeezed states. The corresponding ground-state energy and mean photons agree well with the numerical results for the isotropic and anisotropic coupling cases, while the CS expansions shows a dramatic deviation in the critical regime. Moreover, the quantum fluctuation in the momentum variable is observed by our method.

The paper is organized in the following manner. In Sec. II, we calculate the Wigner function of the wave function

*yuyuzh@cqu.edu.cn
†hzheng@sjtu.edu.cn

numerically. In Sec. III, we develop the CSS expansions to study the ground-state energy and mean photons in the phase transition, and compare to CS expansions. In Sec. V, we study the first-order phase transition of the anisotropic Rabi model by our exact solution. We conclude the paper with a brief discussion.

II. DELOCALIZATION PHASE TRANSITION

The generalized Rabi model describes a two-level atom coupled to a bosonic field with different coupling strengths of the rotating-wave (RW) and counting-rotating-wave (CRW) interactions, which has a wide application in cold atom experiments [38–41]. The isotropic and anisotropic quantum Rabi Hamiltonian is

$$H = \frac{\Delta}{2}\sigma_z + \omega a^\dagger a + g(a^\dagger\sigma_- + a\sigma_+) + g\tau(a^\dagger\sigma_+ + a\sigma_-), \quad (1)$$

where Δ is the transition frequency of a two-level atom, and ω is the frequency of the bosonic field (setting $\omega = 1$). Here $\sigma_i (i = x, y, z)$ are the Pauli matrices, $a^\dagger(a)$ is the creation (annihilation) operator of the boson, and g is the coupling strength, and the relative weight between the RW and CRW interactions is adjusted by the parameter τ. For instance, the isotropic Rabi model corresponds to $\tau = 1$. Due to the CRW interactions, the total excitation number $N = a^\dagger a + \sigma_z/2 + 1/2$ is not conserved and the photon subspace is not closed, rendering a complication of the exact solution in closed form.

The quantum Rabi model has a discrete Z_2 symmetry associated with parity operator $P = e^{i\pi N}$. The parity operator satisfies $[H, P] = 0$ and possesses two eigenvalues $p = \pm 1$ depending on whether the number of quanta is even or odd. The Hilbert space is split in two unconnected subspaces or parity chain, such as $|g\rangle|0\rangle \leftrightarrow |e\rangle|1\rangle \leftrightarrow |g\rangle|2\rangle \leftrightarrow \cdots$ for even parity $p = +1$, and $|e\rangle|0\rangle \leftrightarrow |g\rangle|1\rangle \leftrightarrow |e\rangle|2\rangle \leftrightarrow \cdots$ for even parity $p = -1$. The eigenstate of the system is a superposition of the states in each parity chain. As the coupling strength increases, the ground state includes higher-order states in the parity chain with more photons' excitation, resulting in the increasing of the mean number of photons. In the infinite limit $\Delta/\omega \to \infty$, there occurs the super-radiant phase transition with the symmetry broken at the critical coupling strength $g_c = \sqrt{\Delta\omega}/(1+\tau)$ [10,11]. In this paper, we explore the ground state with the parity symmetry to study critical phenomenons in the scaling limit of $\Delta/\omega = 100$.

It is interesting to explore the essential feature of the wave function associated with the quantum phase transition. Specifically, in the position and momentum (x, p) representation with the operators $x = (a^\dagger + a)/\sqrt{2\omega}$ and $p = i\sqrt{\omega/2}(a^\dagger - a)$, one can observe the distinguished deformations and the symmetry of the wave function in the normal and super-radiant phase. The ground state obtained from numerical diagonalization is of the form

$$|\varphi\rangle = \sum_n^{N_{\rm tr}} |n\rangle(c_{n+}|\widetilde{\uparrow}\rangle + c_{n-}|\widetilde{\downarrow}\rangle), \quad (2)$$

where $c_{n\pm}$ are coefficients, and $N_{\rm tr}$ is the truncated boson number in the Fock space up to 30. $|\widetilde{\uparrow}\rangle$ and $|\widetilde{\downarrow}\rangle$ are the eigenstates of σ_x, giving $|\widetilde{\uparrow}\rangle = (-|\uparrow\rangle + |\downarrow\rangle)/\sqrt{2}$ and $|\widetilde{\downarrow}\rangle = (|\uparrow\rangle + |\downarrow\rangle)/\sqrt{2}$. The position representation of the Fock state of the field $|n\rangle$ are the usual harmonic oscillators

$$\langle x|n\rangle = (\sqrt{\omega}/\sqrt{\pi}2^n n!)^{-1/2} e^{-\omega x^2/2} H_n(\sqrt{\omega}x), \quad (3)$$

where $H_n(\sqrt{\omega}x)$ are Hermite polynomials of order n. Consequently, the wave function in the position representation is

$$|\varphi\rangle = \phi_{+x}|\widetilde{\uparrow}\rangle + \phi_{-x}|\widetilde{\downarrow}\rangle, \quad (4)$$

where the oscillator states in the spin projection is $\phi_{\pm x} = \sum_n c_{n\pm}\langle x|n\rangle$.

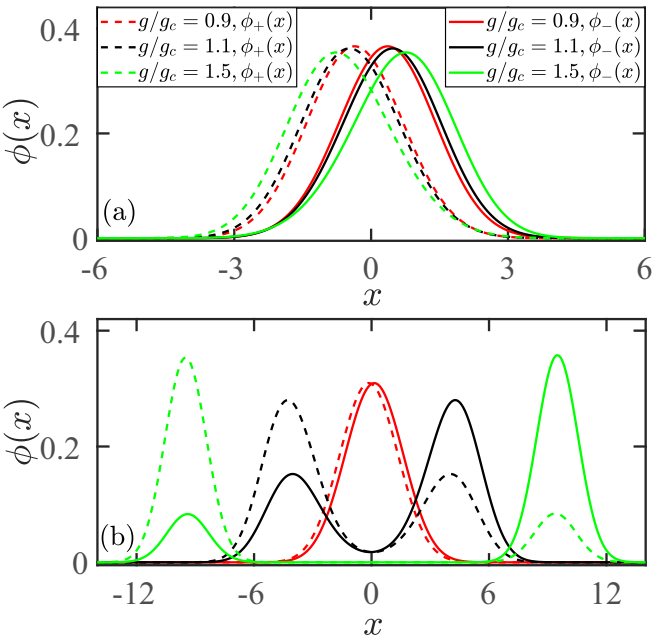

FIG. 1. Wave function of the oscillator states ϕ_{+x} (dashed line) and ϕ_{-x} (solid line) in each spin projection obtained by the exact diagonalization as a function of the position x depending on the scaled coupling strength $g/g_c = 0.9$ (red lines), 1.1 (black lines), and 1.5 (green lines) for different ratio (a) $\Delta/\omega = 1$ and (b) $\Delta/\omega = 100$ for the isotropic Rabi model.

In the case of $\Delta = 0$, the oscillators displace in two directions by projecting onto $|\widetilde{\uparrow}\rangle$ and $|\widetilde{\downarrow}\rangle$. It leads to a doubly degenerate coherent state for the displaced oscillators. For $\Delta/\omega = 1$, two oscillator states ϕ_{+x} and ϕ_{-x} move towards the opposite direction and always have a single peak with a displacement as g/g_c increases in Fig. 1(a). Extending the argument to large ratio $\Delta/\omega = 100$ in Fig. 1(b), the single-peaked wave function stretches and then splits into two when the coupling strength exceeds the critical value $g/g_c = 1.1$, exhibiting an occurrence of the super-radiant phase transition in the infinite-ratio limit. It implies that the oscillator of each spin-projected component becomes delocalized with two displacements of opposite value in the super-radiant phase, which cannot be fulfilled by a single-peak wave packet. Moreover, it is observed that the oscillator states ϕ_{+x} and ϕ_{-x} overlap strongly to form two correlated states. On further increasing the coupling $g/g_c = 1.5$, $\phi_{\pm x}$ moves away from each other and the second peak begins to disappear. It means that two oscillator states $\phi_{\pm x}$ become separated with weak overlap in the deep-strong coupling regime.

The x and p distributions of the oscillator states can be analyzed by the Wigner function, which is introduced in

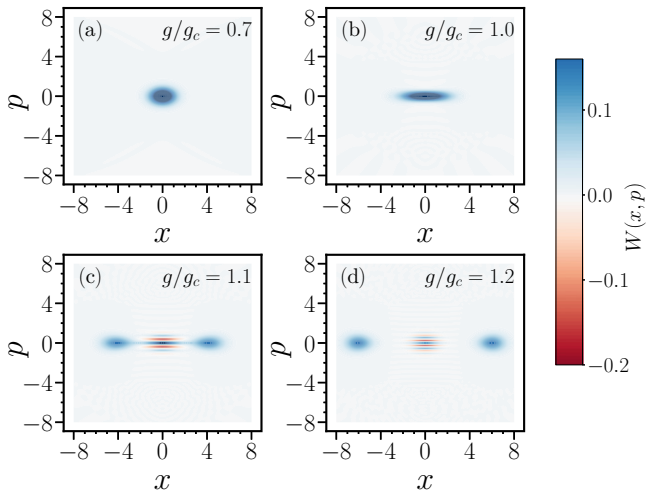

FIG. 2. Wigner function $W(x, p)$ as a function of the momentum p and position x for different coupling strength $g/g_c = 0.7$, 1, 1.1, and 1.2 in the scaling limit of $\Delta/\omega = 100$ for the isotropic Rabi model.

terms of the position and momentum operators $W(x, p) = \frac{1}{2\pi}\int dx'\psi^*(x - \frac{\hbar}{2}x')e^{-ix'p}\psi(x + \frac{\hbar}{2}x')$ [42,43]. From the Fock state in Eq. (2), the reduced density matrix of the oscillator states can be given by tracing out the atom degrees of freedom: $\rho = \mathrm{Tr}_{\mathrm{atom}}|\varphi\rangle\langle\varphi| = \sum_{n,m} c_m c_n^*|m\rangle\langle n|$ with $c_n c_m^* = c_{n+}c_{m+}^* + c_{n-}c_{m-}^*$. The Wigner function can be written explicitly as

$$W(x, p) = \frac{1}{\pi}\int_{-\infty}^{+\infty} e^{2ipx}\sum_{m,n}^{Ntr} c_m c_n^*\langle x - x'|m\rangle\langle n|x + x'\rangle dx'. \quad (5)$$

The transition from the localized to delocalized state with two displacements is clearly observed in Fig. 2. And the squeezing deformations of the oscillator states is found in the momentum space. The squeezing deformations increases as the coupling strengthens and then decreases in the deep-strong coupling regime. Meanwhile, there is an emergence of coherence between two squeezed wave packets around the critical coupling strength g_c. It predicts the correlated delocalized wave function with both of displacement and squeezing deformations in the super-radiant phase.

The key observation is the delocalized state with two correlated and squeezed wave packets above the critical coupling g_c for $\Delta/\omega \to \infty$ in the QRM, which is consistent with that in the Dicke model [44,45]. Due to the finite-ratio effect, the wave function for $\Delta/\omega = 100$ is not divergent around the critical regime, indicating that the corresponding parity symmetry does not break down. Considering the parity symmetry of the wave function, we propose an expansion of the CSS to describe both of the localized and delocalized states.

III. ONE COHERENT-SQUEEZED-STATE ANSATZ

In the normal phase with the coupling strength $g < g_c$, the oscillator state $\phi_{\pm x}$ in each spin projection is formed with a single peak in Fig. 1(b). Due to the displacement and squeezing deformations, the single-peaked wave-function ansatz is described by one coherent-squeezed state (1CSS), which is written as

$$|\psi_{1\mathrm{CSS}}^+\rangle = C_+|\widetilde{\uparrow}\rangle \otimes |+f\rangle_{\mathrm{CSS}} + C_-|\widetilde{\downarrow}\rangle \otimes |-f\rangle_{\mathrm{CSS}}. \quad (6)$$

The oscillator state in each spin projection is described by the CSS

$$|\pm f\rangle_{\mathrm{CSS}} = e^{\beta_\pm(a^\dagger - a)}e^{\xi_\pm(a^2 - a^{\dagger 2})}|0\rangle, \quad (7)$$

with the variational displacements $\beta_\pm$ and the squeezing parameters $\xi_\pm$. Since the ground state is associated with the even parity, satisfying $P|\psi_{1\mathrm{CSS}}^+\rangle = |\psi_{1\mathrm{CSS}}^+\rangle$. It implies the conditions $C_+ = -C_- = 1/\sqrt{2}$, $\beta_+ = -\beta_- = -\beta$, and $\xi_+ = \xi_- = \xi$. This more flexible ansatz facilitates us to obtain the free variables β and ξ.

To compare to the previous coherent state, the ground state with the even parity can be expressed by one coherent state (1CS) as

$$|\psi_{1\mathrm{CS}}^+\rangle = \frac{1}{\sqrt{2}}|+x\rangle \otimes |+f\rangle_{\mathrm{CS}} - \frac{1}{\sqrt{2}}|-x\rangle \otimes |-f\rangle_{\mathrm{CS}}, \quad (8)$$

where the coherent state is

$$|\pm f\rangle_{\mathrm{CS}} = e^{\mp\beta(a^\dagger - a)}|0\rangle. \quad (9)$$

The coherent state includes only the displacement shift $\pm\beta$ by neglecting the squeezing deformations. It can be recovered easily from the coherent-squeezed state $|\pm f\rangle_{\mathrm{CSS}}$ in Eq. (7) by setting $\xi = 0$.

Using the 1CSS ansatz $|\psi_{1\mathrm{CSS}}^+\rangle$, one obtains the energy

$$E_g^{1\mathrm{CSS}} = \omega(\sinh^2 2\xi + \beta^2) - 2\beta\alpha - \left(\frac{\Delta}{2} + 2\gamma\beta\eta^2\right)e^{-2\beta^2\eta^2}, \quad (10)$$

with parameters $\alpha = g(1 + \tau)/2$, $\gamma = g(\tau - 1)/2$, and $\eta = \cosh(2\xi) - \sinh(2\xi)$. Similarly, the energy $E_g^{1\mathrm{CS}}$ for the 1CS ansatz $|\psi_{1\mathrm{CS}}^+\rangle$ is given easily by setting $\xi = 0$ in Eq. (10)

The oscillator displacement β and squeezing variable ξ can be determined by minimizing the energy $E_g^{1\mathrm{CSS}}$. The variational energy $E_g^{1\mathrm{CSS}}$ is minimized according to $\partial E_g^{1\mathrm{CSS}}/\partial\beta = 0$ and $\partial E_g^{1\mathrm{CSS}}/\partial\xi = 0$, respectively. For instance, one obtains the equations for the isotropic case $\tau = 1$

$$\omega(e^{4\xi} - e^{-4\xi}) - 4\Delta\beta^2 e^{-4\xi}e^{-2\beta^2\eta^2} = 0, \quad (11)$$

$$(\omega\beta - g) + \Delta\beta e^{-4\xi}e^{-2\beta^2\eta^2} = 0. \quad (12)$$

In the limit $\Delta/\omega \to \infty$, the optimal displacement and squeezing variables are given approximately

$$\beta \simeq \frac{g}{\Delta}, \xi \simeq \frac{1}{8}\ln\left(1 + \frac{g^2}{g_c^2}\right). \quad (13)$$

It demonstrates that the displacement β tends to be 0 in the infinite limit. The squeezing variable ξ begins to become increasingly dependent on the coupling strength. The displacement and squeezing deformations are consistent with those in Figs. 2(a) and 2(b).

Figures 3(a) and 3(b) show the ground-state energy $E_g^{1\mathrm{CSS}}$ obtained by 1CSS in the normal phase, which agrees well with the numeric ones for the isotropic $\tau = 1$ and anisotropic $\tau = 1.5$ cases. However, there are noticeable deviations of the energy $E_g^{1\mathrm{CS}}$ for 1CS as the coupling strength approaches to

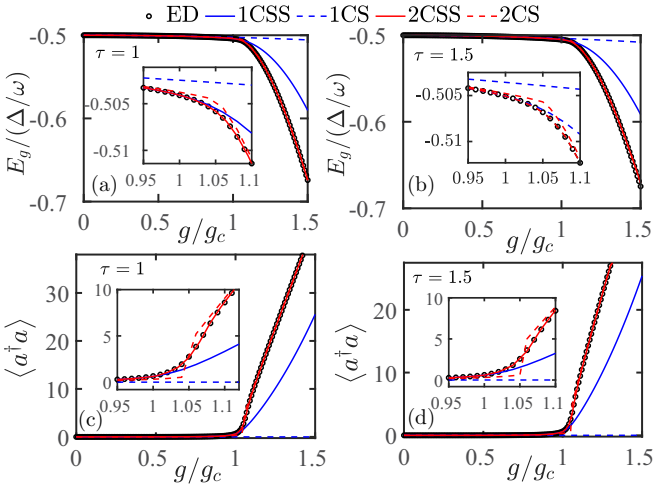

FIG. 3. Ground-state energy $E_g/(\Delta/\omega)$ and mean photon number $\langle a^\dagger a\rangle$ for one coherent-squeezed state (1CSS) (blue solid lines) and two coherent-squeezed state (2CSS) (red solid lines) as a function of the rescaled coupling strength g/g_c for the (a, c) isotropic $\tau = 1$ and (b, d) anisotropic $\tau = 1.5$ cases in the scaling limit of $\Delta/\omega = 100$. The results obtained by exact diagonalization (ED) (circles), one coherent state (1CS) (blue dashed lines), and two coherent state (2CS) (red dashed lines) are listed for comparison. The inset shows the results around the critical value from $g/g_c = 0.95$ to 1.1.

the critical value g_c. The failure of the 1CS is that the squeezing effect is underestimated. Around the critical regime, the contribution of the squeezing becomes significant and should be considered.

To explore the validity of the wave function, we calculate the mean photons by the 1CSS ansatz

$$\langle\psi^+_{\text{1CSS}}|a^\dagger a|\psi^+_{\text{1CSS}}\rangle = \sinh^2(2\xi) + \beta^2. \tag{14}$$

The 1CSS results agree well with the numerics ones in the normal phase in Figs. 3(c) and 3(d). However, the 1CS with only the displacement shows an obvious deviation around the critical value. Note that the mean photon $\langle a^\dagger a\rangle$ is macroscopically excited above g_c, and higher-order excitations are required. The 1CSS fails to describe the exact wave function for the multiphoton process in the super-radiant phase.

IV. TWO COHERENT-SQUEEZED-STATE ANSATZ

As the coupling strength exceeds the critical value, the spin-projected oscillators $\phi_\pm$ begins to overlap strongly in Fig. 1(b), resulting in two correlated Gaussians of the wave packets. The strong-correlated physics motivates the inclusion of the second CSS for each oscillator state. As an improvement, the ground state ansatz $|\psi^+_{\text{2CSS}}\rangle$ is proposed by a linear combination of two coherent-squeezed state (2CSS)

$$\begin{aligned}|\psi^+_{\text{2CSS}}\rangle = |\widetilde{\uparrow}\rangle \otimes (C_1|+f_1\rangle_{\text{CSS}} + C_2|+f_2\rangle_{\text{CSS}}) \\ - |\widetilde{\downarrow}\rangle \otimes (C_1|-f_1\rangle_{\text{CSS}} + C_2|-f_2\rangle_{\text{CSS}}),\end{aligned} \tag{15}$$

where each coherent-squeezed state is given by $|\pm f_k\rangle_{\text{CSS}} = e^{\mp\beta_k(a^\dagger - a)}e^{\xi(a^2 - a^{\dagger 2})}|0\rangle$. The symmetry of the even parity enforces the chosen relative sign between the spin components

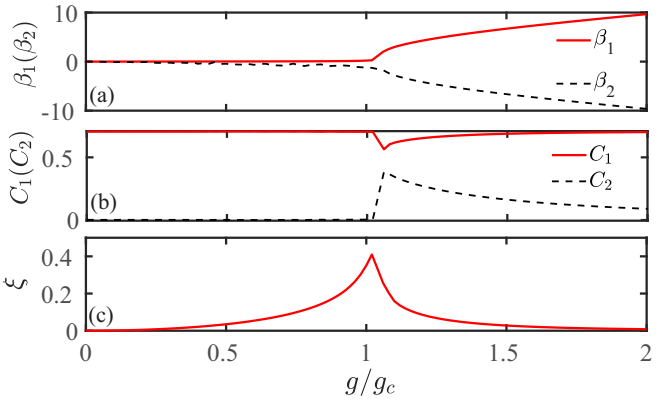

FIG. 4. (a) Displacement variables β_1 (red solid line) and β_2 (black dashed line), (b) the coefficients C_1 (red solid line) and C_2 (black dashed line), (c) and the squeezing ξ using the wave function $|\psi^+_{\text{2CSS}}\rangle$ for the isotropic Rabi model in the scaling limit of $\Delta/\omega = 100$.

$|\widetilde{\uparrow}\rangle$ and $|\widetilde{\downarrow}\rangle$ of the state in Eq. (15). Normalization of $|\psi^+_{\text{2CSS}}\rangle$ gives the condition

$$1 = 2C_1^2 + 2C_2^2 + 2C_1C_2(\langle+f_1|+f_2\rangle + \langle-f_1|-f_2\rangle), \tag{16}$$

where the overlap of two coherent-squeezed states is

$$\langle+f_1|\pm f_2\rangle = \langle-f_1|\mp f_2\rangle = e^{-\eta^2(\beta_1\mp\beta_2)^2/2}. \tag{17}$$

Variables $C_{1(2)}$, $\beta_{1(2)}$, and ξ are taken as free parameters and can be determined by minimizing the energy $E_g^{\text{2CSS}} = \langle\psi^+_{\text{2CSS}}|H|\psi^+_{\text{2CSS}}\rangle$ in the Appendix. By neglecting the squeezing effects with $\xi = 0$, it recovers the two-peaked wave function $|\psi^+_{\text{2CS}}\rangle$ with two coherent states (2CS).

Figure 3 shows the ground-state energy E_g^{2CSS} and mean photon $\langle a^\dagger a\rangle$ obtained by the 2CSS ansatz $|\psi^+_{\text{2CSS}}\rangle$. The superradiance of photons is observed by the mean photon, which begins to increase dramatically above the critical value. Excellent agreement between the results of 2CSS and numerical ones is exhibited in the whole coupling regimes. The 2CSS ansatz makes great improvement on the 1CSS by adding the second coherent-squeezed state, which corresponds to higher-order excitations in the super-radiant phase. However, the 2CS with only the variable displacement deviates from numerical results around g_c.

Since the first two-level term of the Hamiltonian in Eq. (1) does not commute with the interaction part, it leads to higher-order excitations for the multiphoton process for the strong coupling, such as a^2 and $a^{\dagger 2}$ [30,31]. The CS expansion with only the displacement transformation fails to describe such quadratic terms. The nontrivial squeeze effects in the CSS approach are account for the effective nonlinear interactions. Moreover, the advantage of the 2 CSS expansion lies in contributions from the second coherent-squeezed state, which originates from the higher-order excitations and the enhancement of the overlap of oscillators around g_c.

Figure 4 shows the variables $\beta_{1(2)}$, $C_{1(2)}$, and squeezing parameter ξ for the 2CSS ansatz, which are calculated by minimizing the ground-state energy E_g^{2CSS}. In the normal phase with $g/g_c < 1$, the coefficient C_1 approaches to $1/\sqrt{2}$ and C_2 tends to 0, which recovers to 1CSS ansatz for the single-peaked wave function. As coupling exceeds the critical

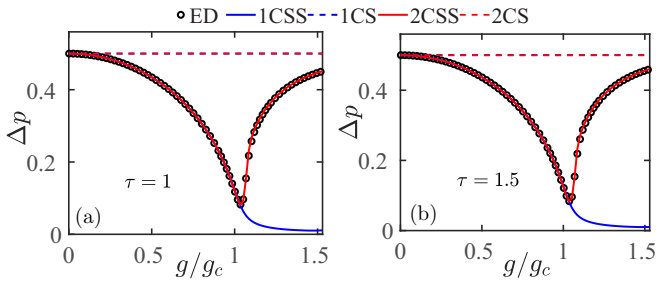

FIG. 5. The variance of the momentum Δp in the ground state as a function of the rescaled coupling strength g/g_c obtained by the 1CSS (blue solid lines) and 2CSS (red solid lines) for the (a) isotropic $\tau = 1$ and (b) anisotropic $\tau = 1.5$ coupling cases. The results obtained by ED (circles), 1CS (blue dashed lines), and 2CS (red dashed lines) are listed for comparison.

value, C_2 increases dramatically and the additional second coherent-squeezed state plays a crucial role in lowering the ground-state energy. It corresponds to the occurrence of the second peak of the two-peaked wave function for $g/g_c = 1.1$ in Fig. 1(b). With further increase of g/g_c, the probability of the second peak $|C_2|^2$ decreases, which is consistent with the vanishing of the second peaks for $g/g_c = 1.5$ in Fig. 1(b).

Meanwhile, the displacements of two oscillators states β_1 and $|\beta_2|$ are approximated to be 0 in the normal phase, and increase dramatically as the coupling strength exceeds the critical value. The squeezing parameter ξ increases to the maximum value at g_c, and then decreases in the deep-strong coupling regime. The squeezing effects are qualitatively observed from the squeezed wave packets in the momentum space by the Winger function in Fig. 2.

To explore the squeezed momentum variance in the phase transition, we calculate the variance of the momentum $\Delta p = \langle p^2\rangle - \langle p\rangle^2$. A sharp drop of the momentum variance is observed at g_c in Fig. 5, which indicates that the momentum quadrature for the exact wave function is squeezed. The variance Δp obtained by the 1CS equals a constant $\omega/2$ independent on the coupling strength [28], and there is no squeezing effects even for the 2CS. In contrast to the failure of the CS expansion, the 2CSS successfully captures the squeezing variance of the momentum, exhibiting the reduced quantum fluctuations in the momentum variable in the phase transition.

V. FIRST-ORDER QUANTUM PHASE TRANSITION IN THE ANISOTROPIC RABI MODEL

For the anisotropic Rabi model, in addition the second-order phase transition, an additional first-order phase transition occurs at the critical value $g_c^{(1)} = \sqrt{\Delta\omega/(1-\tau^2)}$ [38]. When the RW coupling strength becomes stronger than that of the CRW terms, e.g., $\tau < 1$, there exists an energy-level crossing between the ground state and the first-excited state. A natural question follows as to the ground-state wave function in the first-order phase transition. Due to the energy-level crossing, the even parity symmetry of the ground state breaks down and the first-excited state with the odd parity becomes the lowest-energy state.

The first-excited state with the odd parity can be expressed by the linear superposition of two coherent-squeezed

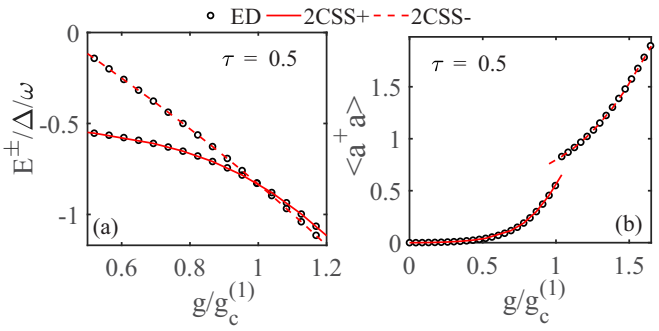

FIG. 6. (a) Energy levels $E^{\pm}$ for the ground state $|\psi^{+}_{2\mathrm{CSS}}\rangle$ (red solid line) and the first-excited state $|\psi^{-}_{2\mathrm{CSS}}\rangle$ (red dashed line) as a function of the scaled coupling strength $g/g_c^{(1)}$ for the anisotropic case $\tau = 0.5$. Numerical results by the exact diagonalization are listed (black circle) for comparison. (b) Mean photon number $\langle a^{\dagger}a\rangle$ in the ground state as a function of $g/g_c^{(1)}$.

states

$$|\psi^{-}_{2\mathrm{CSS}}\rangle = |\widetilde{\uparrow}\rangle \otimes (C_1|+f_1\rangle_{2\mathrm{CSS}} + C_2|+f_2\rangle_{2\mathrm{CSS}}) + |\widetilde{\downarrow}\rangle \otimes (C_1|-f_1\rangle_{2\mathrm{CSS}} + C_2|-f_2\rangle_{2\mathrm{CSS}}). \quad (18)$$

The parity operator satisfies $P|\psi^{-}_{2\mathrm{CSS}}\rangle = -|\psi^{-}_{2\mathrm{CSS}}\rangle$. Different from $|\psi^{+}_{2\mathrm{CSS}}\rangle$ in Eq. (15) with the even parity symmetry, the first-excited state $|\psi^{-}_{2\mathrm{CSS}}\rangle$ changes the sign of the wave function for the spin part $|\widetilde{\downarrow}\rangle$ due to the odd parity. For the first-order phase transition, the ground state undergoes a transition from $|\psi^{+}_{2\mathrm{CSS}}\rangle$ with the even parity to $|\psi^{-}_{2\mathrm{CSS}}\rangle$ with the odd parity at the critical value $g_c^{(1)}$.

The energies for the ground state and first-excited state can be obtained as $E^{\pm} = \langle\psi^{\pm}_{2\mathrm{CSS}}|H^{\mathrm{Rabi}}|\psi^{\pm}_{2\mathrm{CSS}}\rangle$ (see the Appendix), respectively. The variational displacement, squeezing parameter, and coefficients can be determined by minimizing the energy $E_g^{\pm}$.

Figure 6(a) shows energy levels $E^{\pm}$ for the ground state $|\psi^{+}_{2\mathrm{CSS}}\rangle$ and the first-excited state $|\psi^{-}_{2\mathrm{CSS}}\rangle$, which agree well with the numerical ones. Energy-levels crossing is captured correctly at the critical value $g_c^{(1)}$ by the 2CSS expansion. Meanwhile, the average photons $\langle a^{\dagger}a\rangle$ in the ground state show a discontinuous transition in Fig. 6(b), which ascribes to the parity broken in the first-order phase transition. With the even and odd parities, the 2CSS expansion can accurately describe the ground state and the first-excited state for arbitrary coupling strengths.

VI. CONCLUSION

We find that the wave function in the super-radiant phase is delocalized with two-peaked wave packets, which is distinguished from the one-peaked wave packet in the normal phase. The additional squeezing deformations of the exact wave function in the momentum space are observed besides the displacement shift by the Wigner function. With these deformations, we develop the coherent-squeezed-state expansion to describe the ground state for each phases correctly, exhibiting excellent agreement of the ground-state energy and the mean photons with numerical ones. Moreover, the reduced quantum fluctuation in the momentum variable is correctly captured by our improved method, exhibiting the

improvement over the coherent-state expansion with only displacement transformation. The success of our method lies in the inclusion of the squeezing effects and the second coherent-squeezed state, which accounts for the higher-order excitations resulting in nonlinear effects in the phase transition. Our method provides an intuitive understanding of the wave function for the quantum phase transition in many-body systems of greater complexity.

ACKNOWLEDGMENTS

The authors thank Qing-Hu Chen for useful discussions. The work was supported in part by the National Natural Science Foundation of China (Grants No. 11874260 and No. 11847301), NSAF (Grant No. U1930403), and by the Fundamental Research Funds for the Central Universities (Grants No. 2019CDXYWL0029 and No. 2019CDJDWL0005).

APPENDIX: ENERGY DEVIATION FOR THE TWO COHERENT-SQUEEZED STATE

For the two coherent-squeezed state $|\psi^{+}_{2\mathrm{CSS}}\rangle$ with the even parity in Eq. (15) and $|\psi^{-}_{2\mathrm{CSS}}\rangle$ with the odd parity in Eq. (18), the energy is expressed by $E^{\pm} = \pm E^{\mathrm{atom}} + E^{ph} + E^{\mathrm{iso\text{-}int}} \pm E^{\mathrm{ani\text{-}int}}$, which consists of

$$\begin{aligned} E^{\mathrm{atom}} &= \left\langle \psi^{+}_{2\mathrm{CSS}} \middle| \frac{\Delta}{2}\sigma_z \middle| \psi^{+}_{2\mathrm{CSS}} \right\rangle \\ &= -\Delta\big(C_1^2\langle +f_1|-f_1\rangle + 2C_1C_2\langle +f_1|-f_2\rangle + C_2^2\langle +f_2|-f_2\rangle\big), \end{aligned} \tag{A1}$$

$$\begin{aligned} E^{ph} &= \langle \psi^{+}_{2\mathrm{CSS}}|\omega a^{\dagger}a|\psi^{+}_{2\mathrm{CSS}}\rangle \\ &= \omega\big[2C_1^2\beta_1^2 + 2C_2^2\beta_2^2 + 2C_1C_2\beta_1\beta_2(\langle +f_1|+f_2\rangle + \langle -f_1|-f_2\rangle)\big] \\ &\quad +\omega\sinh^2\xi\big\{2C_1^2 + 2C_2^2 + C_1^2e^{-2\beta_1^2\eta^2} + C_2^2e^{-2\beta_2^2\eta^2} \\ &\quad +2C_1C_2[1-\eta^2(\beta_1-\beta_2)^2](\langle +f_1|+f_2\rangle + \langle -f_1|-f_2\rangle)\big\} \\ &\quad +\omega\sinh\xi[2C_1C_2\eta(\beta_1-\beta_2)^2(\langle +f_1|+f_2\rangle + \langle -f_1|-f_2\rangle)], \end{aligned} \tag{A2}$$

$$\begin{aligned} E^{\mathrm{iso\text{-}int}} &= \langle \psi^{+}_{2\mathrm{CSS}}|\alpha(a^{\dagger}+a)\sigma_x|\psi^{+}_{2\mathrm{CSS}}\rangle \\ &= -2\alpha[C_1^2\beta_1 + C_2^2\beta_2 + C_1C_2(\beta_1+\beta_2)\big(\langle +f_1|+f_2\rangle + \langle -f_1|-f_2\rangle)], \end{aligned} \tag{A3}$$

$$\begin{aligned} E^{\mathrm{ani\text{-}int}} &= \langle \psi^{+}_{2\mathrm{CSS}}|\gamma(a^{\dagger}-a)i\sigma_y|\psi^{+}_{2\mathrm{CSS}}\rangle \\ &= -4\gamma\eta^2\big[C_1^2\beta_1\langle +f_1|-f_1\rangle + C_1C_2(\beta_1+\beta_2)\langle +f_1|-f_2\rangle + C_2^2\beta_2\langle +f_2|-f_2\rangle\big]. \end{aligned} \tag{A4}$$

[1] I. I. Rabi, Phys. Rev. **51**, 652 (1937).
[2] D. Nagy, G. Kónya, G. Szirmai, and P. Domokos, Phys. Rev. Lett. **104**, 130401 (2010).
[3] F. Dimer, B. Estienne, A. S. Parkins, and H. J. Carmichael, Phys. Rev. A **75**, 013804 (2007).
[4] A. Wallraff, D. I. Schuster, A. Blais, L. Frunzio, R.-S. Huang, J. Majer, S. Kummar, S. M. Girvin, and R. J. Schoelkopf, Nature (London) **431**, 162 (2004).
[5] T. Niemczyk, F. Deppe, H. Huebl, E. P. Menzel, F. Hocke, M. J. Schwarz, J. J. Garcia-Ripoll, D. Zueco, T. Hümmer, E. Solano, A. Marx, and R. Gross, Nat. Phys. **6**, 772 (2010).
[6] P. Forn-DÍaz, J. J. GarcÍa-Ripoll, B. Peropadre, J.-L. Orgiazzi, M. A. Yurtalan, R. Belyansky, C. M. Wilson, and A. Lupascu, Nat. Phys. **13**, 39 (2016).
[7] F. Yoshihara, T. Fuse, S. Ashhab, K. Kakuyanagi, S. Saito, and K. Semba, Nat. Phys. **13**, 44 (2017).
[8] X. Gu, A. F. Kockum, A. Miranowicz, Y. X. Liu, and F. Nori, Phys. Rep. **718**, 1 (2017).
[9] A. F. Kockum, A. Miranowicz, S. D. Liberato, S. Savasta, and F. Nori, Nat. Rev. Phys. **1**, 19 (2019).
[10] M. J. Hwang, R. Puebla, and M. B. Plenio, Phys. Rev. Lett. **115**, 180404 (2015).
[11] M. X. Liu, S. Chesi, Z. J. Ying, X. S. Chen, H. G. Luo, and H. Q. Lin, Phys. Rev. Lett. **119**, 220601 (2017).
[12] L. T. Shen, Z. B. Yang, H. Z. Wu, and S. B. Zheng, Phys. Rev. A **95**, 013819 (2017).
[13] R. H. Dicke, Phys. Rev. **93**, 99 (1954).
[14] N. Lambert, C. Emary, and T. Brandes, Phys. Rev. Lett. **92**, 073602 (2004).
[15] Q. H. Chen, Y. Y. Zhang, T. Liu, and K. L. Wang, Phys. Rev. A **78**, 051801(R) (2008).
[16] X. Y. Lu, L. L. Zheng, G. L. Zhu, and Y. Wu, Phys. Rev. App. **9**, 064006 (2018).
[17] Y. Xu and H. Pu, Phys. Rev. Lett. **122**, 193201 (2019).
[18] D. Braak, Phys. Rev. Lett. **107**, 100401 (2011).
[19] Q. H. Chen, C. Wang, S. He, T. Liu, and K. L. Wang, Phys. Rev. A **86**, 023822 (2012).
[20] H. H. Zhong, Q. T. Xie. M. T. Batchelor, and C. H. Li, J. Phys. A **41**, 415302 (2013).
[21] E. K. Irish, Phys. Rev. Lett. **99**, 173601 (2007).
[22] Y. Y. Zhang, Q. H. Chen, and Y. Zhao, Phys. Rev. A **87**, 033827 (2013).
[23] C. J. Gan and H. Zheng, Eur. Phys. J. D **59**, 473 (2010).

[24] Y. Zhang, G. Chen, L. Yu, Q. Liang, J.-Q. Liang, and S. Jia, Phys. Rev. A **83**, 065802 (2011).
[25] S. Agarwal, S. M. Hashemi Rafsanjani, and J. H. Eberly, Phys. Rev. A **85**, 043815 (2012).
[26] S. Ashhab, Phys. Rev. A **87**, 013826 (2013).
[27] L. W. Duan, Y. F. Xie, D. Braak, and Q. H. Chen, J. Phys. A: Math. Theor. **49**, 464002 (2016).
[28] X. Y. Chen and Y. Y. Zhang, Phys. Rev. A **97**, 053821 (2018).
[29] L. Cong, X. M. Sun, M. X. Liu, Z. J. Ying, and H. G. Luo, Phys. Rev. A **99**, 013815 (2019).
[30] Y. Y. Zhang, Phys. Rev. A **94**, 063824 (2016).
[31] Y. Y. Zhang and X. Y. Chen, Phys. Rev. A **96**, 063821 (2017).
[32] T. Shi, J. Q. Pan, and S. Yi, arXiv:1909.02432.
[33] F. H. Maldonado-Villamizar, C. Huerta Alderete, and B. M. Rodríguez-Lara, Phys. Rev. A **100**, 013811 (2019).
[34] B. Gao, G. X. Li, and Z. Ficek, Phys. Rev. A **94**, 033854 (2016).
[35] H. B. Shore and L. M. Sander, Phys. Rev. B **7**, 4537 (1973).
[36] Z. J. Ying, M. X. Liu, H. G. Luo, H. Q. Lin, and J. Q. You, Phys. Rev. A **92**, 053823 (2015).
[37] S. Bera, S. Florens, H. U. Baranger, N. Roch, A. Nazir, and A. W. Chin, Phys. Rev B **89**, 121108(R) (2014).
[38] Q.-T. Xie, S. Cui, J.-P. Cao, L. Amico, and H. Fan, Phys. Rev. X **4**, 021046 (2014).
[39] Y. Y. Xiang, J. W. Ye, and W.-M. Liu, Sci. Rep. **3**, 3476 (2013).
[40] K. Baumann, C. Guerlin, F. Brennecke, and T. Esslinger, Nature (London) **464**, 1301 (2010).
[41] A. T. Black, H. W. Chan, and V. Vuletic, Phys. Rev. Lett. **91**, 203001 (2003).
[42] U. Leonhardt and H. Paul, *Measuring the Quantum State of Light* (Cambridge University Press, Cambridge, England, 1997).
[43] J. R. Johansson, P. D. Nation, and F. Nori, Comput. Phys. Commun. **183**, 1760 (2012).
[44] T. Liu, Y. Y. Zhang, Q. H. Chen, and K. L. Wang, Phys. Rev. A **80**, 023810 (2009).
[45] C. Emary and T. Brandes, Phys. Rev. E **67**, 066203 (2003).